Hindawi
Journal of Advanced Transportation
Volume 2022, Article ID 8348726, 20 pages
https://doi.org/10.1155/2022/8348726

Research Article

Modeling and Simulation of Traffic Congestion for Mixed Traffic Flow with Connected Automated Vehicles: A Cell Transmission Model Approach

Yunxia Wu,[1,2] Yalan Lin,[1,3,4] Rong Hu,[1,3,4] Zilan Wang,[1,3,4] Bin Zhao,[1,3,4] and Zhihong Yao [1,3,4]

[1]*School of Transportation and Logistics, Southwest Jiaotong University, Chengdu, Sichuan 610031, China*
[2]*Faculty of Geosciences and Environmental Engineering, Southwest Jiaotong University, Chengdu, Sichuan 611756, China*
[3]*National Engineering Laboratory of Integrated Transportation Big Data Application Technology, Southwest Jiaotong University, Chengdu, Sichuan 611756, China*
[4]*National United Engineering Laboratory of Integrated and Intelligent Transportation, Southwest Jiaotong University, Chengdu, Sichuan 611756, China*

Correspondence should be addressed to Zhihong Yao; zhyao@swjtu.edu.cn

Received 13 May 2022; Revised 2 June 2022; Accepted 9 June 2022; Published 27 June 2022

Academic Editor: Zhenzhou Yuan

Connected automated vehicles (CAVs) can significantly shorten the headway of car following, thereby effectively improving the traffic capacity and injecting new power to alleviate traffic congestion. To investigate the congestion characteristics of mixed traffic flow with CAVs and human-driven vehicles (HDVs), this paper proposes a cell transmission model to capture and simulate traffic congestion for mixed traffic flow. Firstly, the Newell, adaptive cruise control (ACC), and cooperative adaptive cruise control (CACC) models are adopted to capture the car-following behavior of different vehicles. Secondly, the fundamental diagram under different penetration rates of CAVs is derived based on car-following models. Then, the cell transmission model (CTM) of mixed traffic flow is developed based on the classical CTM and fundamental diagram of mixed traffic flow. Finally, two simulation methods, mixed traffic flow CTM and micro-simulation, are designed to verify the effectiveness of the proposed model. Moreover, taking the moving bottleneck on the expressway as an example, the congestion characteristics of mixed traffic flow are analyzed using multiple indexes, such as average travel speed, congestion delay, and congestion scale. The results show the following: (i) CAVs can significantly alleviate traffic congestion, (ii) the duration of the bottleneck is positively correlated with the degree of traffic congestion, and (iii) The traffic congestion assessment results under different model parameters slightly differ, but the impact is negligible.

1. Introduction

With the rapid development of technology and automobile globalization, the increase in car ownership has led to increasingly severe traffic congestion, resulting in traffic accidents, personal and property safety, and economic losses [1–5]. As an emerging technology in the environment of a new round of technological revolution, connected automated vehicles (CAVs) can realize vehicle-to-vehicle communication and vehicle-to-infrastructure cooperation with the help of onboard monitoring systems and advanced information terminal technology [6–10]. Therefore, collaborative control and intelligent decision-making among CAVs can be realized in the future [11].

At present, CAVs have entered a stage of rapid development worldwide. Many countries such as Europe and the United States have introduced related policies for CAVs. These policies put forward the direction of the development of the industry of CAVs and strengthen the actual road test of CAVs. At the same time, Volvo, Mercedes Benz, Audi, Tesla, and other foreign car companies can achieve L2-level automatic driving. Some car companies are expected to

commercialize L4-level automated driving in the future [12]. However, CAVs are still in the stage of large-scale implementation, which will ultimately replace traditional human-driven vehicles (HDVs). Therefore, the vehicles on the road will present a mixed traffic flow of manual HDVs and CAVs.

For the research of mixed traffic flow with CAVs and HDVs, some scholars [13–15] used microscopic models, such as the cellular automata model and car-following model, to describe mixed traffic flow under different CAVs penetration rates. These studies mainly focus on analyzing the congestion characteristics, traffic safety, and traffic efficiency of mixed traffic flow with CAVs and HDVs. The results showed that CAVs could effectively improve traffic capacity and significantly alleviate traffic congestion. However, most of the research mainly uses the micro-simulation method. Micro-simulation can simulate the operation of traffic flow more accurately, but it has some disadvantages, such as difficulty in calibrating parameters and low efficiency. As a meso-level model, the cell transmission model (CTM) is rarely used to analyze the characteristics of mixed traffic flow under different CAVs penetration rates. Moreover, only a few studies consider the car-following degradation phenomenon of CAVs. Therefore, considering the car-following degradation phenomenon of CAVs, this paper proposes a cell transmission model to model and simulate traffic congestion for mixed flow with CAVs and HDVs. The main contributions are as follows:

(1) For the mixed traffic flow composed of different types of vehicles such as HDVs, adaptive cruise control (ACC) vehicles, and cooperative adaptive cruise control (CACC) vehicles, we analyze the degradation of CAVs and derive the fundamental diagram of mixed traffic flow under different CAVs penetration rates.

(2) To analyze the congestion characteristics of mixed traffic flow from the meso level, this paper extracts the model parameters under different CAVs penetration rates through the fundamental diagram of mixed traffic flow. Then, we propose the CTM of mixed traffic flow to quickly and accurately analyze the traffic congestion phenomenon and its characteristics.

(3) The average travel speed, congestion delay, and congestion scale are selected to verify the effectiveness and accuracy of the proposed model based on a simulation.

The rest of this paper is organized as follows: The research on mixed traffic flow modeling and congestion analysis in the CAVs environment is reviewed in Section 2. Section 3 derives the fundamental diagram of mixed traffic flow based on the microscopic car-following model. Then, the CTM model of mixed traffic flow is constructed, and the congestion indexes are used to evaluate traffic congestion. Section 4 simulates traffic congestion scenarios and carries out sensitivity analysis. Section 5 finally draws the research conclusions and future works of this paper.

2. Literature Review

To alleviate the traffic congestion effectively, some scholars have explored the mechanism of traffic flow operation [16–19]. Daganzo [20] first proposed the CTM model in 1994, which studied traffic flow characteristics on highways with single entrance and exit. In 1995, the network traffic flow was discussed by this method. The research proved that CTM could describe the phenomenon of vehicle queuing well and reflect the characteristics of traffic dynamics [21]. Dong et al. [22] used the improved CTM to reflect the principle of traffic congestion in the regional traffic network. They estimated the spatial diffusion of traffic congestion by predicting traffic congestion time to capture secondary congestion accurately. The experimental results showed that the model predicted the duration of traffic congestion effectively and accurately. Carey et al. [23] established a traffic flow operation model based on the CTM, considering the multilane and lane change conditions. The model clarified the lane-changing and congestion characteristics under single- and multilane conditions. Canudas-de-Wit and Ferrara and Ferrara [24] designed a new macroscopic traffic model with variable cell length to analyze the road system composed of three state variables. The model described the propagation characteristics of traffic congestion and verified the best steady-state speed under traffic conditions. Considering the interaction of different vehicle types, Qian et al. [25] constructed a macro heterogeneous traffic flow model to simulate the characteristics of mixed traffic flow, including free flow, semicongestion, and complete congestion. Therefore, the studies mentioned above prove that scholars have many research achievements on classical CTM and improved CTM. Moreover, CTM is widely used in traffic flow analysis and traffic simulation. The main reason is that CTM can accurately and efficiently describe traffic flow characteristics. The simulation result can explain traffic flow's complex phenomena and evolution rules in the road traffic network. Therefore, CTM is an important method to reveal the mechanism of traffic flow operation.

With the development of CAVs, there are many research results on mixed traffic flow in CAVs environment. These studies include the macro and micro characteristics of traffic flow, traffic assignment, and road intersection [8, 26–30]. Yuan et al. [14] used a cellular automaton (CA) model to simulate a mixed traffic flow composed of ACC vehicles and HDVs. Then, they analyzed the characteristics of the mixed traffic flow in three different states: free flow, synchronous flow, and congested flow. Combining qualitative and quantitative methods to compare the probability of traffic congestion, they proved that ACC vehicles had a particular impact on the state of traffic congestion. Zheng et al. [31] defined a mixed traffic flow composed of HDVs and CAVs through a stochastic model and analyzed the driving behavior of CAVs to HDVs and the stability of traffic flow. The simulation results showed that under the high CAVs penetration rate, the uncertainty of manual driving behavior was effectively reduced, and mixed traffic flow stability was improved. Ye and Yamamoto [13] established a heterogeneous mixed traffic flow model through the simulation

Table 1: Overview of traffic flow modeling and congestion analysis.

Author, year	Research level	Vehicle types	Considered CAVs degradation
Daganzo, 1994 [20]	Macro level	(1) HDV	×
Dong et al., 2012 [22]	Macro level	(1) HDV	×
Carey et al., 2015 [23]	Macro level	(1) HDV	×
Canudas-de-Wit and Ferrara, 2018 [24]	Macro level	(1) HDV	×
Qian et al., 2017 [25]	Macro level	(1) HDV	×
Yuan et al., 2009 [14]	Micro level	(1) HDV, (2) ACC	×
Zheng et al., 2020 [31]	Micro level	(1) HDV, (2) AVs	×
Ye and Yamamoto, 2019 [13]	Micro level	(1) HDV, (2) CACC	×
Zhu et al., 2020 [15]	Micro level	(1) HDV, (2) ACC, (3) CACC	√
Qin et al., 2017; Qin et al., 2018; Qin et al., 2018 [32–34]	Micro level	(1) HDV, (2) ACC, (3) CACC	√
Jiang et al., 2020 [35]	Micro level	(1) HDV, (2) CAVs	×
Ramezani and Ye, 2019 [36]	Macro level	(1) HDV, (2) CACC	×
Xu et al., 2020 [37]	Micro level	(1) HDV, (2) CAVs	×
This paper	Meso level	(1) HDV, (2) ACC, (3) CACC	√

analysis of the mixed traffic flow composed of HDVs and CAVs. Then, they studied the differences in acceleration, speed distribution, and safety under different CAVs penetration rates. The results showed that CAVs could enhance the stability of the overall traffic flow and reduce the risk of traffic accidents. Zhu [15] considered the influence of driver personality differences on traffic congestion and the capacity of mixed traffic flow. Then, numerical simulation simulated the mixed traffic flow composed of HDVs, ACC, and CACC. The results showed that cautious drivers and CACC vehicles were more conducive to smooth traffic and effectively reduced instability frequency. Qin et al. [32–34] studied the stability and safety of mixed traffic flow in the CAVs environment based on the front vehicle feedback condition and derived the fundamental diagram of mixed traffic flow. Then, the stability of mixed traffic flow and different CAVs penetration rates was analyzed. Taking the stability and safety of mixed traffic flow as the research object, Jiang et al. [35] adopted the car-following model to study the traffic flow characteristics under different CAVs penetration rates. Considering that automated vehicles (AVs) can provide more flexible centralized and decentralized control schemes, Ramezani and Ye [36] developed a lateral flow-control strategy for AVs to alleviate traffic congestion. A two-level control scheme was constructed to optimize lane density distribution and reflect lane change. Simulation experiments were used to verify the effectiveness of the control scheme, which provided a scientific and effective theoretical reference for the practical application of AVs. Xu et al. [37] simulated the scene of the mixed traffic flow by VISSIM software. Considering the influence of reaction time, they derived a fundamental diagram of mixed traffic flow and analyzed the traffic capacity under different CAVs penetration rates. The above studies had thoroughly investigated the operating characteristics of mixed CAVs traffic flow in various traffic scenarios, but most studies focused on the micro level. Moreover, only a few studies consider the car-following degradation phenomenon of CAVs.

According to Table 1, there are three gaps in the existing research: (1) the research on the mixed traffic flow is mainly based on the micro level and macro level, which rarely from the meso level to analyze the characteristics of mixed traffic flow with CAVs; (2) CAVs are divided into different technical levels, and only a few of them consider the car following degradation phenomenon of CAVs; (3) most of them only use the average travel speed to evaluate the congestion characteristics of mixed traffic flow, and the evaluation index is too single.

3. Methodology

Based on a cell transmission model approach, this paper aims to model and simulate traffic congestion for mixed flow with CAVs and HDVs. The research framework of this paper is shown in Figure 1.

3.1. Car-Following Behavior. Vehicles on the road are composed of HDVs and CAVs, and CAVs are divided into two types: ACC vehicles and CACC vehicles. In a mixed traffic flow, if the front vehicle of the CAV is an HDV, the CAV will not be able to communicate with it because HDV does not have a communication function. Therefore, the CAV communication function will degrade at this time, as shown in Figure 2. Assuming that there are n vehicles in the mixed traffic flow, the ratio of CAVs and HDVs is p: μ, where $p + \mu = 1$. As a result, the proportion of ACC vehicles in CAVs is $p\mu$, and the ratio of CACC vehicles is $p - p\mu = p^2$. To sum up, the proportions of the three types of vehicles in the mixed traffic flow are as follows:

$$\begin{cases} P_{\mathrm{HDV}} = \mu, \\ P_{\mathrm{ACC}} = p\mu, \\ P_{\mathrm{CACC}} = p^2, \end{cases} \tag{1}$$

where P_{HDV}, P_{ACC}, and P_{CACC} represent the proportion of HDVs, ACC vehicles, and CACC vehicles in mixed traffic flow, respectively.

3.1.1. Human-Driven Vehicles. As the CAV is in the popularization stage, the vehicles on the road are still dominated by traditional HDVs. The HDV is the conventional vehicle

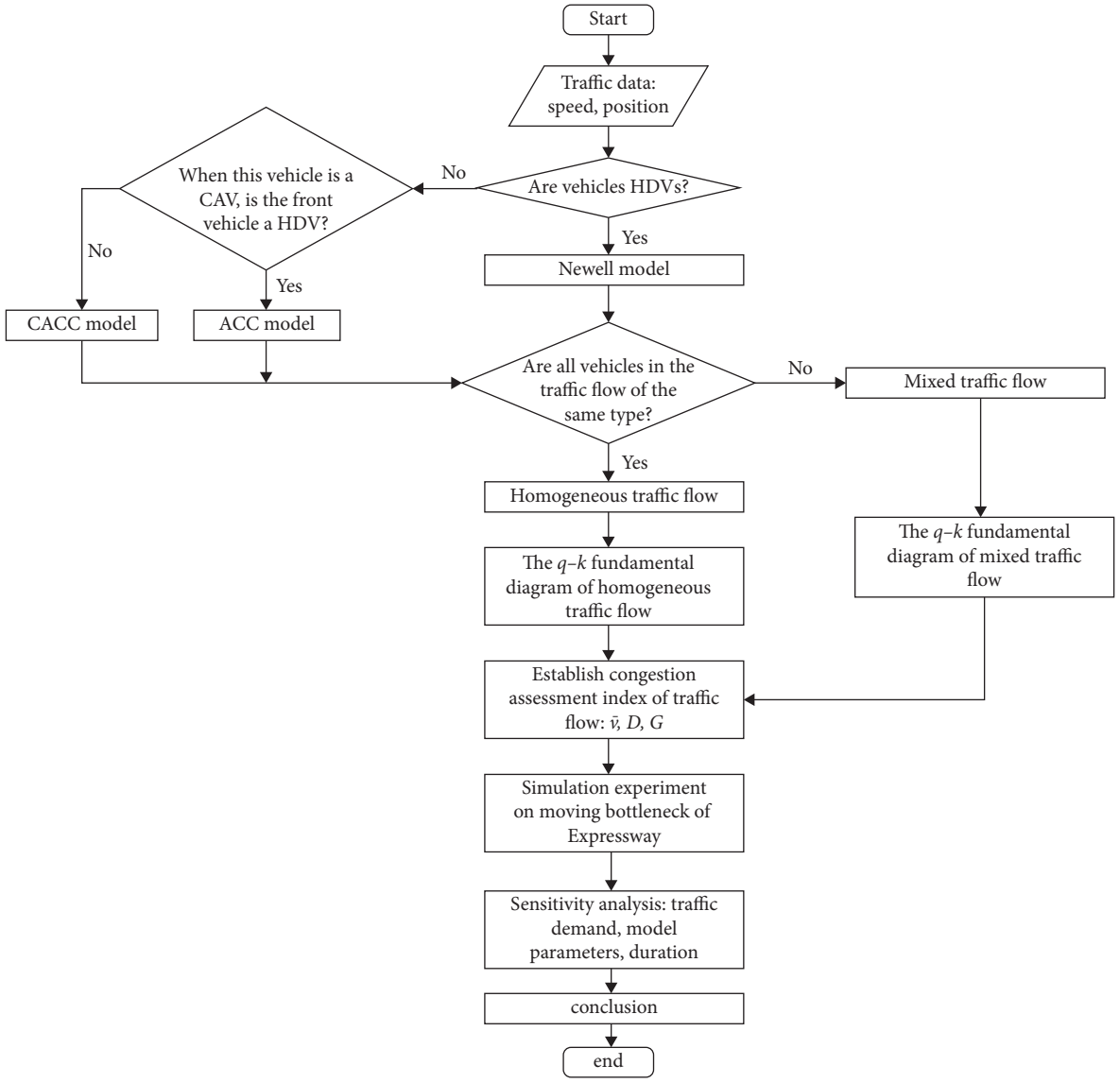

Figure 1: The framework of this paper.

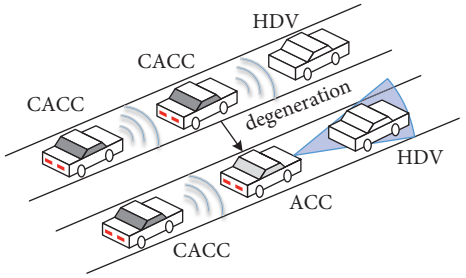

Figure 2: Car-following degradation in mixed traffic flow.

controlled by the driver, which only knows the road traffic environment and the surrounding vehicle information through the driver's human sense. A variety of micro car-following models are currently applied to the simulation of HDVs, such as the Newell model [18], optimal velocity model (OVM) [16], full velocity difference (FVD) model [38], and intelligent driver model (IDM) [39]. To facilitate the construction of the proposed model, the linear Newell model is selected to describe the car following the behavior of HDVs.

Newell [18] proposed the Newell model, which is a car-following model with time delay by using front and following vehicle displacement control. Its mathematical model is

$$x_n\left(t + t_H\right) = x_{n-1}\left(t\right) - L_H, \tag{2}$$

where $x_n(t + t_H)$ is the position of HDVs after the t_H delay time, $x_{n-1}(t)$ indicates the position of the $n-1$ HDV at the time t, and L_H is the displacement difference in HDVs. After parameter calibration [40], its value is $t_H = 1.5s$ and $L_H = 7m$.

3.1.2. Connected Automated Vehicles. Compared with HDVs, CAVs have certain advantages in driving. ACC vehicle refers to a vehicle equipped with an ACC system,

which judges the road driving condition through the onboard monitoring unit and monitors and captures the running information of the front vehicle in real time. Therefore, ACC vehicles can play a role in assisting the driver and reducing the driving burden. ACC model is a car following model calibrated by the actual data of PATH laboratory, which is more consistent with the driving characteristics of ACC vehicles. Therefore, this paper adopts the ACC model [41, 42] to capture the car following characteristics of ACC vehicles in mixed traffic flow. Its mathematical formula is

$$\dot{v_n}(t) = k_1\left[h_n(t) - l - s_0 - t_A v_n(t)\right] + k_2\Delta v, \tag{3}$$

where k_1 and k_2 are the control parameter of the model; $v_n(t)$ is the speed of vehicle n at the time t; $h_n(t)$ is the space headway between the vehicle n and the vehicle in front at the time t; l is the vehicle length, taken as 5 m; s_0 is the minimum distance at a standstill, which is set as 2 m; s_0 is the constant time interval expected to be maintained by ACC vehicles; and Δv is the speed difference between the front and rear vehicles. According to the actual vehicle test of PATH laboratory [41], the calibration results of the ACC model parameter are $k_1 = 0.23\text{s}^{-2}$ and $k_2 = 0.07\text{s}^{-1}$, while the t_A parameter values are 1.1 s, 1.6 s, and 2.2 s with the acceptance ratios of 50.4%, 18.5%, and 31.1%, respectively.

CACC vehicles are expanding based on ACC vehicles, which can realize vehicle-to-vehicle communication. In addition, CACC vehicles effectively form a platoon of CAVs, significantly improving vehicles' driving efficiency and making traffic systems more intelligent, informative, and collaborative. The CACC model of the PATH laboratory can effectively reduce the headway between vehicles, thereby improving the capacity of road traffic. Therefore, the CACC model is used to simulate and present the driving characteristics of CACC vehicles in a mixed traffic flow. The mathematical expression of the CACC model [41, 42] is

$$\begin{cases} v_n(t) = v_p + k_p e_n + k_d \dot{e_n}(t), \\ e_n = h_n(t) - l - s_0 - t_C v_n(t), \end{cases} \tag{4}$$

where v_p is the speed of the last control time; k_p and k_d are the control parameters of the model; e_n is the space headway error of vehicle n at the time t, and its derivative form is $\dot{e_n}(t)$; and t_C is the expected time headway for CACC vehicles. According to the literature [41], parameter calibration is carried out through actual data, and the calibration results are $k_p = 0.45$ and $k_d = 0.25$, while the t_C parameter values are 0.6 s, 0.7 s, 0.9 s, and 1.1 s with the acceptance ratios of 57%, 24%, 7%, and 12%, respectively.

3.2. Fundamental Diagram

3.2.1. Fundamental Diagram of Homogeneous Traffic Flow. According to Section 3.1, when the traffic flow is homogeneous with all HDVs, the Newell model is adopted to capture the car-following behavior of HDVs. Then, the relationship between headway and speed in the equilibrium state is as follows [18]:

$$\begin{cases} x_n(t) = x_{n-1}(t) - h_H^*, \\ x_n(t + t_H) = x_n(t) + v^* t_H, \end{cases} \tag{5}$$

where h_H^* is the space headway of HDVs in a balanced state and v^* is the speed of HDVs in a balanced state.

Taking equation (5) into equation (2), the headway of HDVs in the balanced state is obtained as follows:

$$h_H^* = v^* t_H + L_H. \tag{6}$$

According to the relationship between headway and traffic density in the equilibrium state, the traffic density of homogeneous traffic flow composed of only HDVs is calculated as follows:

$$\begin{aligned} k_H^* &= \frac{1}{h_H^*} \\ &= \frac{1}{v^* t_H + L_H}, \end{aligned} \tag{7}$$

where k_H^* is the traffic density of HDVs in a balanced state.

Therefore, from equation (7), the volume-speed fundamental diagram corresponding to the homogeneous traffic flow of HDVs is obtained as follows:

$$\begin{cases} k_H = \dfrac{1}{v^* t_H + L_H}, \\ q_H = k_H v, \end{cases} \tag{8}$$

where q_H is the traffic volume of HDVs in a balanced state.

For the homogeneous traffic flow composed of all ACC vehicles, the speed difference and acceleration between the front and rear vehicles in the ACC model are all 0. The equilibrium headway h_A^* in the homogeneous traffic flow composed of ACC vehicles [43, 44] is

$$h_A^* = v^* t_A + l + s_0. \tag{9}$$

Similarly, the equilibrium headway h_C^* under the homogeneous traffic flow composed of CACC vehicles [43, 44] is calculated as follows:

$$h_C^* = v^* t_C + l + s_0. \tag{10}$$

Let $L_A = l + s_0$ and $L_C = l + s_0$ in equations (9) and (10), which are simplified as follows:

$$\begin{cases} h_A^* = v^* t_A + L_A, \\ h_C^* = v^* t_C + L_C. \end{cases} \tag{11}$$

According to the relationship between traffic density and headway, the volume-density fundamental diagrams corresponding to the ACC and CACC traffic flow are derived from equations (10) and (11).

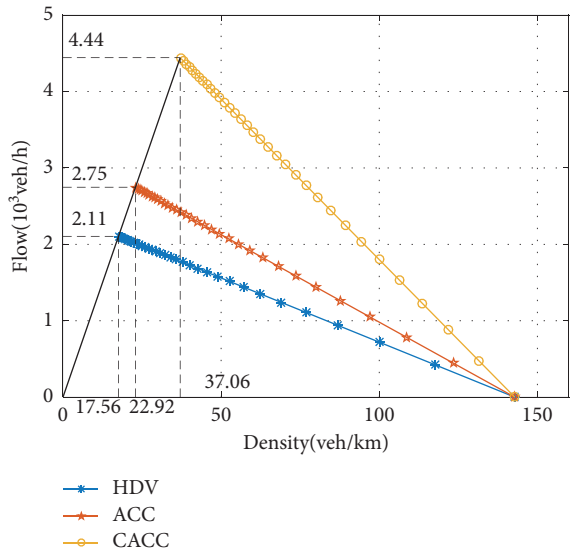

Figure 3: Fundamental diagram of homogeneous traffic flow under different vehicle types.

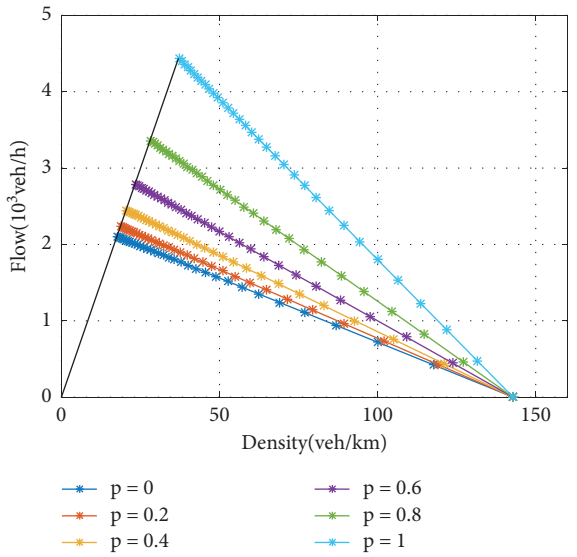

Figure 4: Fundamental diagram of mixed traffic flow under different CAVs penetration rates.

$$\begin{cases} k_A = \dfrac{1}{v^* t_A + L_A}, \\ q_A = k_A v, \end{cases} \tag{12}$$

$$\begin{cases} k_C = \dfrac{1}{v^* t_C + L_C}, \\ q_C = k_C v. \end{cases} \tag{13}$$

Based on the volume-density fundamental diagram of homogeneous traffic flow, taking $t_A = 1.1s$ and $t_C = 0.6s$ as an example, the volume-density curves of homogeneous traffic flow under different vehicle types are drawn, as shown in Figure 3.

Figure 3 shows that the maximum capacity of HDV, ACC, and CACC traffic flow is 2,110 veh/h, 2,750 veh/h, and 4,440 veh/h, respectively, and the corresponding optimum density is 17.56 veh/km, 22.92 veh/km, and 37.06 veh/km, respectively. Therefore, the capacity of the CACC traffic flow is the largest, while the capacity of the HDVs traffic flow is the smallest. Moreover, the maximum capacity of the HDVs traffic flow is less than 1/2 of the maximum capacity of the CACC traffic flow.

3.2.2. Fundamental Diagram of Mixed Traffic Flow. Mixed traffic flow comprises three types of vehicles, including HDVs, ACC vehicles, and CACC vehicles. The difference from the homogeneous traffic flow is that the headway of the homogeneous traffic flow is the same in the balanced state, but the balance headway between the different types of vehicles in the mixed traffic flow is different.

Therefore, by taking the proportion of different vehicles in equation (1) into equations (6) and (11), the average headway of mixed traffic flow in the equilibrium state is obtained.

$$h^* = \frac{nP_{\mathrm{HDV}} h_H^* + nP_{\mathrm{ACC}} h_A^* + nP_{\mathrm{CACC}} h_C^*}{n}, \tag{14}$$

where h^* is the average headway of vehicles in the mixed traffic flow in the equilibrium state.

Similarly, based on the relationship between headway and traffic density, the traffic density of mixed traffic flow in the equilibrium state is obtained.

$$k^* = \frac{1}{h^*} = \frac{1}{P_{\mathrm{HDV}}(vt_H + L_H) + P_{\mathrm{ACC}}(vt_A + L_A) + P_{\mathrm{CACC}}(vt_C + L_C)}, \tag{15}$$

where k^* is the density of mixed traffic flow in the equilibrium state.

From the change of equation (15), the speed of mixed traffic flow in the equilibrium state is expressed as follows:

$$v^* = \frac{1}{k(P_{\mathrm{HDV}} t_H + P_{\mathrm{ACC}} t_A + P_{\mathrm{CACC}} t_C)} - \frac{P_{\mathrm{HDV}} L_H + P_{\mathrm{ACC}} L_A + P_{\mathrm{CACC}} L_C}{P_{\mathrm{HDV}} t_H + P_{\mathrm{ACC}} t_A + P_{\mathrm{CACC}} t_C}. \tag{16}$$

According to the relationship between traffic flow parameters, the fundamental diagram of mixed traffic flow under different CAVs penetration rates is represented.

$$q^* = \frac{1}{P_{\mathrm{HDV}} t_H + P_{\mathrm{ACC}} t_A + P_{\mathrm{CACC}} t_C} - k\frac{P_{\mathrm{HDV}} L_H + P_{\mathrm{ACC}} L_A + P_{\mathrm{CACC}} L_C}{P_{\mathrm{HDV}} t_H + P_{\mathrm{ACC}} t_A + P_{\mathrm{CACC}} t_C}, \tag{17}$$

where q^* is the flow of mixed traffic flow in the equilibrium state.

Table 2: Key parameters of the fundamental diagram under different CAV penetration rates.

Penetration rate	Maximum capacity ($q_{\max}$)	Critical density (k_c)	The percentage increase of $q_{\max}$ (based on $p=0$)
$p = 0$	2.105	17.559	—
$p = 0.2$	2.236	18.650	6.21%
$p = 0.4$	2.449	20.426	16.32%
$p = 0.6$	2.790	23.275	32.55%
$p = 0.8$	3.364	28.060	59.80%
$p = 1$	4.443	37.065	111.08%

For the fundamental diagram of mixed traffic flow derived from equation (17), taking $t_A = 1.1s$, $t_C = 0.6s$ as an example, the fundamental diagram of mixed traffic flow is shown in Figure 4. The vehicles in the mixed traffic flow are all HDVs when the CAV penetration rate is $p = 0$, while all the vehicles in the mixed traffic flow are CACC vehicles when the CAV penetration rate is $p = 1$. However, when the penetration rate of CAVs p is between 0 and 1, CACC vehicles degenerate into ACC vehicles in the mixed traffic flow; that is, the traffic flow is composed of three types of vehicles.

Figure 4 indicates that the maximum capacity and critical density are different under different CAVs penetration rates. The road has a higher maximum capacity under a high CAV penetration rate, which shows that CAVs can improve the road's traffic capacity. The maximum capacity $q_{\max}$ and critical density k_c under different CAV penetration rates are shown in Table 2. As shown in Figure 4 and Table 2, when the CAV penetration rate is $0 < p < 0.6$, the maximum capacity increases with the increase of the penetration rate, and the growth rate is slow. Furthermore, when the CAV penetration rate is greater than 0.6, the maximum capacity is greatly improved by increasing the CAV penetration rate. The increased percentage of $q_{\max}$ is only 32.55% when the CAV penetration rate is 0.6, while the increasing percentage of $q_{\max}$ is far more than twice that of the CAV penetration rate $p = 0$. This is because when the penetration rate is lower than 0.6, HDVs and ACC vehicles account for the main part of the mixed traffic flow, so the maximum capacity increases slowly. However, when the penetration rate exceeds 0.6, CACC vehicles account for the main part of the mixed traffic flow. Moreover, CACC's headway is relatively small, effectively improving traffic capacity.

The reason is that when the CAVs penetration rate is $p > 0$, the mixed traffic flow contains HDVs and CAVs, so the CAVs following the HDVs degenerate from CACC vehicles to ACC vehicles. Moreover, ACC vehicles increase the instability of traffic flow in the car following degradation. The expected headway of ACC vehicles is 1.1s, which is not significantly different from that of HDVs. Therefore, the increase in ACC vehicles has no significant effect on improving traffic capacity.

3.3. Mixed Flow Cell Transmission Model. The difference from the classic CTM is that the vehicles transmitted between cells in the mixed traffic flow CTM are a mixture of HDVs and CAVs. It is no longer a single vehicle type, so it is necessary to respecify the model parameters under different CAVs penetration rates. The model parameters include the maximum capacity $q_{\max}$ between two adjacent cells, the congestion density k_{jam}, and the backward wave velocity ω. Therefore, based on the fundamental diagram of mixed traffic flow constructed in Section 3.2, the parameter values of the mixed traffic flow CTM are obtained.

Equation (15) shows that when the speed is $v = v_f$, the critical density k_c of mixed traffic flow is denoted as follows:

$$k_c = \frac{1}{P_{\text{HDV}}\left(v_f t_H + L_H\right) + P_{\text{ACC}}\left(v_f t_A + L_A\right) + P_{\text{CACC}}\left(v_f t_C + L_C\right)}. \tag{18}$$

Similarly, when the speed is $v = 0$, the traffic congestion density reaches the maximum, so the congestion density k_{jam} is as follows:

$$k_{\text{jam}} = \frac{1}{P_{\text{HDV}} L_H + P_{\text{ACC}} L_A + P_{\text{CACC}} L_C}. \tag{19}$$

Moreover, combined with the relationship of traffic flow parameters and equation (18), the maximum capacity of mixed traffic flow is calculated as follows:

$$q_{\max} = \frac{1}{v_f\left[P_{\text{HDV}}\left(v_f t_H + L_H\right) + P_{\text{ACC}}\left(v_f t_A + L_A\right) + P_{\text{CACC}}\left(v_f t_C + L_C\right)\right]}. \tag{20}$$

In addition, according to the principle of the fundamental diagram, the backward wave velocity of mixed traffic flow is calculated by equations (18)–(20).

$$\omega = -\frac{P_{\text{HDV}} L_H + P_{\text{ACC}} L_A + P_{\text{CACC}} L_C}{P_{\text{HDV}} t_H + P_{\text{ACC}} t_A + P_{\text{CACC}} t_C}. \tag{21}$$

The CTM is the approximate discrete value of the LWR model of the macroscopic traffic dynamics model, which can quickly and efficiently solve the model. Daganzo [20] discretized the continuous traffic flow in time and space based on the mathematical theory of cellular automata, which divided the road sections into cells with equal length.

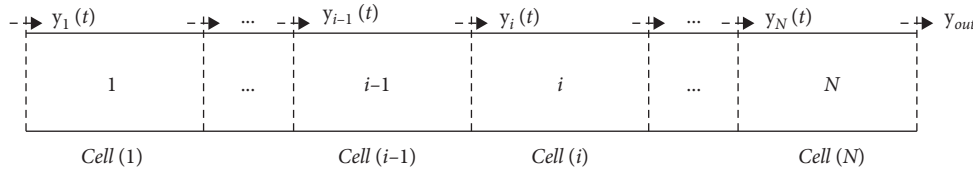

Figure 5: The principle of traffic flow propagation between cells on basic road sections.

Moreover, the length of cells is generally not less than the distance of standard vehicles in a control time step under a free-flow state. The traffic flow propagation between cells is shown in Figure 5.

Suppose the simulation interval is δ and the cell length is Δl (where $\Delta l = v_f \times \delta$) [20]. The mathematical recurrence relation of the cell update on the basic road section is

$$m_i(t+\delta) = m_i(t) + y_i(t) - y_{i+1}(t), \tag{22}$$

where $m_i(t+\delta)$ is the number of vehicles in cell i at the end time in the t-th time interval, $m_i(t)$ is the number of vehicles in cell i at the initial time in the t-th time interval, and $y_i(t)$ is the number of vehicles flowing from cell $i-1$ to cell i in the t-th time interval.

The vehicles transmitted between cells are HDVs, ACC, and CACC vehicles in the mixed traffic flow. The maximum capacity of the mixed traffic flow and the maximum number of vehicles allowed in cells are affected by P_{HDV}, P_{ACC}, and P_{CACC}. Therefore, when the traffic flow transmitted by the cell is composed of different types of vehicles, the maximum capacity of the cell is

$$Q_{\max} = \frac{\Delta x}{P_{\mathrm{HDV}}\left(v_f t_H + L_H\right) + P_{\mathrm{ACC}}\left(v_f t_A + L_A\right) + P_{\mathrm{CACC}}\left(v_f t_C + L_C\right)}. \tag{23}$$

The maximum number of vehicles a cell can hold is expressed as follows:

$$\begin{aligned} M &= k_{\mathrm{jam}} \Delta x \\ &= \frac{\Delta x}{\{P_{\mathrm{HDV}} L_H + P_{\mathrm{ACC}} L_A + P_{\mathrm{CACC}} L_C\}}. \end{aligned} \tag{24}$$

Based on the classical CTM, from equations (23) and (24), it can be concluded that the propagation relationship of the cell in mixed traffic flow is

$$y_i(t) = \min\left\{m_{i-1}(t), Q_{\max}\Delta t, -\frac{\omega}{v_f}\left(M - m_i(t)\right)\right\}. \tag{25}$$

Moreover, cell propagation is divided into two parts: cell outflow and cell inflow. Therefore, it is deduced from equations (23) and (24) that the maximum sending and receiving capacity of the cell under the mixed traffic flow is

$$\begin{cases} S_{i-1}(t) = \min\{m_{i-1}(t), Q_{\max}\Delta t\}, \\ R_i(t) = \min\left\{Q_{\max}\Delta t, -\dfrac{\omega}{v_f}\left(M - m_i(t)\right)\right\}, \end{cases} \tag{26}$$

where $S_{i-1}(t)$ is the maximum number of vehicles that cell $i-1$ can flow out in the t-th time interval and $R_i(t)$ is the maximum number of vehicles that can be accepted by cell i in the t-th time interval.

To sum up, the CTM of mixed traffic flow can be described in equations (22)–(26).

3.4. Congestion Evaluation Indexes. To evaluate traffic congestion, it is necessary to select some evaluation indexes, which can capture traffic congestion accurately and effectively. The principle of choosing the indexes must be objective, scientific, and comparable. However, a single congestion index only reflects a one-sided traffic congestion state but cannot fully provide comprehensive feedback on all aspects of the traffic flow state. Therefore, this paper selects average travel speed, congestion delay, and congestion scale as evaluation indexes.

The travel speed refers to the ratio of the length of the road passed by the vehicle to the travel time required [45]. The average travel speed refers to the ratio of the average travel time of all vehicles passing through the road segment. Therefore, the average travel speed is defined as follows:

$$\overline{v} = \frac{Nl}{\sum_{i=1}^{n} t_i}, \tag{27}$$

where $\overline{v}$ is the average travel speed, l is the length of the road segment, and N is the number of vehicles in the road segment. The higher the average travel speed is, the smoother the traffic flow is. On the contrary, the lower the index value is, the worse the operation effect is, and the more serious the traffic congestion is.

Congestion delay is the difference between the number of vehicles that flow out of a cell in a simulation time interval and flow out in a time step in the free-flow state [45]. The congestion delay of cell i at the t-th simulation time is expressed as follows:

$$d_i(t) = m_i(t) - y_{i+1}(t), \tag{28}$$

where $d_i(t)$ is the congestion delay of the i-th cell at the t-th simulation time.

By summing up the congestion delays of all cells, the total delay of the road segment is obtained as follows:

$$D = \sum_i d_i(t), \tag{29}$$

where D is the total congestion delay of the road segment.

The congestion scale is the ratio of the number of the congested road segment to the total road segments [45]. In this study, the road is divided into cells. Therefore, we define

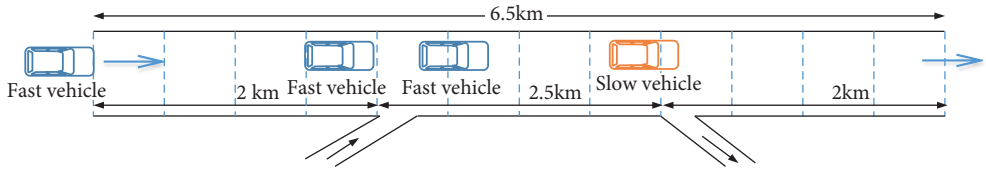

Figure 6: Simulation scenario.

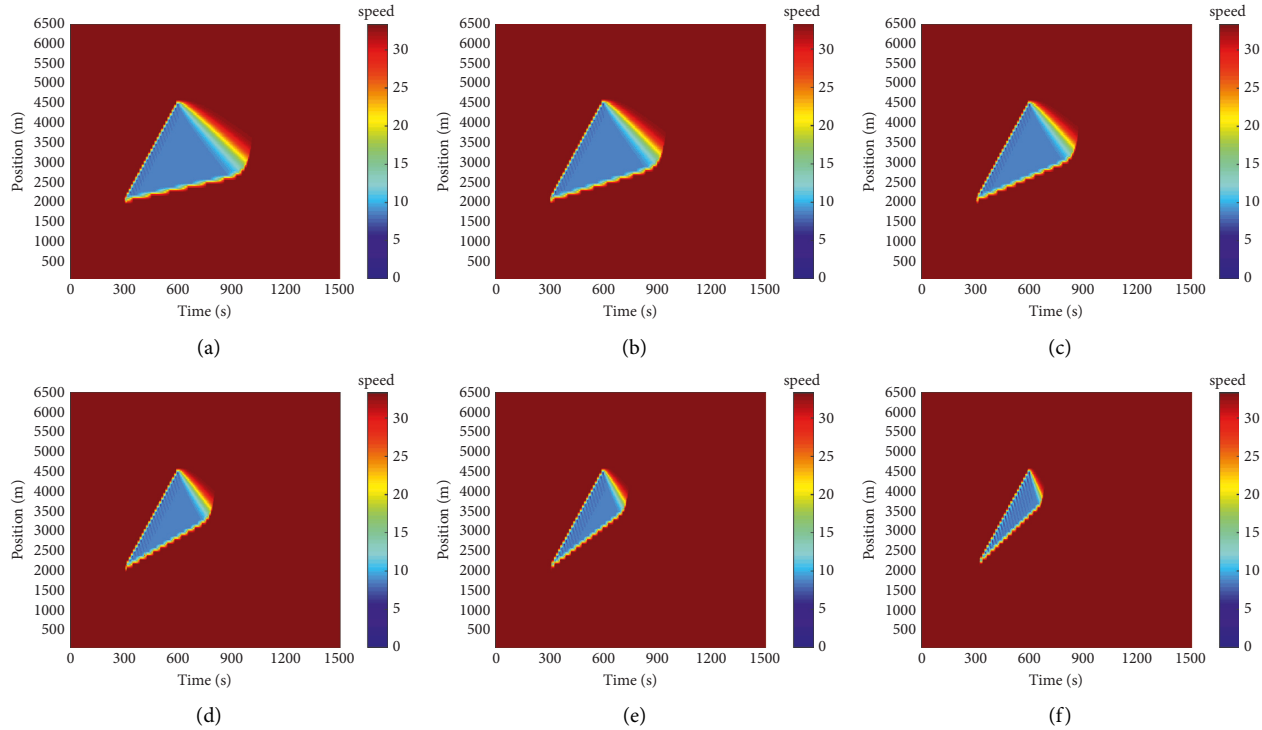

Figure 7: Speed heat map based on CTM model of mixed traffic flow: (a) $p = 0$, (b) $p = 0.2$, (c) $p = 0.4$, (d) $p = 0.6$, (e) $p = 0.8$, and (f) $p = 1$.

the congested cell as the cell density that exceeds the density of free flow. The ratio of the number of congested cells to the total number of cells is used to capture traffic congestion. The congestion scale is

$$G = \frac{M_c}{M_T}, \tag{30}$$

where G is the congestion scale of the road segment, M_c is the number of congested cells in the road segment, and M_T is the total number of cells in the road segment.

4. Case Study and Results

4.1. Simulation Settings. To verify the feasibility of the model, the microscopic car-following model and the mixed traffic flow CTM are adapted to simulate the same traffic scene. The results of the two simulation methods are compared to verify the effectiveness of the model. To avoid the influence of model parameters, the expected headway in the two simulation methods remains the same, that is, $t_H = 1.5s, t_A = 1.1s$, and $t_C = 0.6s$. A moving bottleneck is taken as a case study, a one-way highway with a length of 6.5 km. The merging ramp is located at the road length of 2 km, while the diverging ramp is situated at 4.5 km. The merging ramp and the diverging ramp are single lanes, as shown in Figure 6.

Each vehicle enters from the upstream of the highway with a speed of 120 km/h, while the vehicle speed in the ramp area is 30 km/h. When the vehicle from the ramp area joins the main road at the 300-th second of the simulation time, its speed is significantly lower than that of the main road, thus forming a moving bottleneck. The traffic demand of the main road is 1,400 veh/h, and the HDVs and CAVs randomly enter the simulation road according to the CAV penetration rate. The total time of the simulation experiment is 1,500 s, and the time interval is 3 s. The moving bottleneck of the highway starts from 300 s to 600 s, which lasts for 300 s.

4.2. Result Analysis

4.2.1. Simulation Results Based on the CTM Model. The road segment is divided into 65 cells with 100 m growth based on the principle of the CTM model. The mixed traffic flow CTM model is used to simulate the moving bottleneck and explore the change law of traffic congestion under different CAV

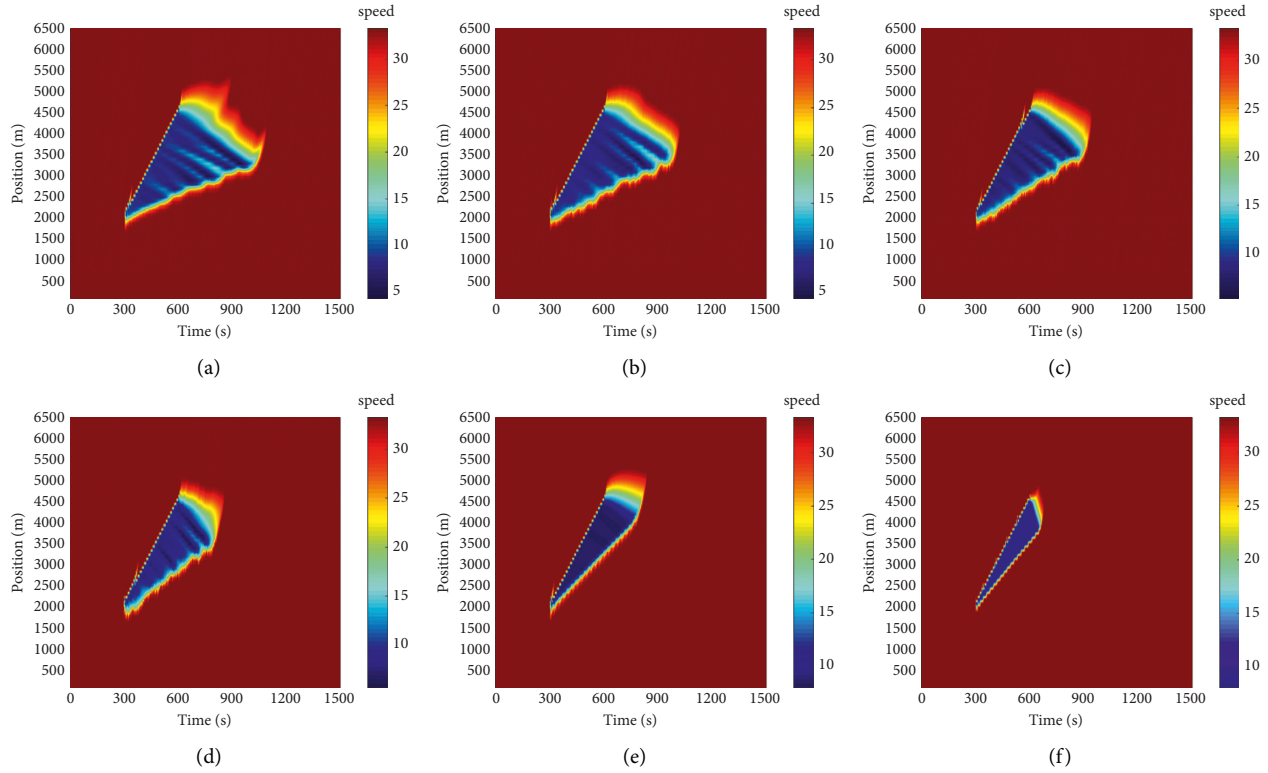

Figure 8: Speed heat map based on the car-following model: (a) $p = 0$, (b) $p = 0.2$, (c) $p = 0.4$, (d) $p = 0.6$, (e) $p = 0.8$, and (f) $p = 1$.

Table 3: Comparison of simulation results under two simulation methods.

Penetration rate	Congestion impact time of CTM simulation (s)	Congestion impact time of micro-simulation (s)	Error	Relative error (%)
0	651	679	28	4.12
0.2	597	637	40	5.89
0.4	525	547	22	3.24
0.6	453	461	8	1.18
0.8	390	399	9	1.33
1	333	340	7	1.03

penetration rates. When the CAV penetration rates are 0, 0.2, 0.4, 0.6, 0.8, and 1, respectively, the simulation speed heat map is shown in Figure 7.

Figure 7 shows the required time for the congestion to dissipate under different CAVs penetration rates. In Figure 7(a), the HDV is a human-controlled vehicle that requires a certain length of reaction phase; thus, traffic congestion needs a longer time to dissipate. From Figures 7(a), 7(d), and 7(e), the application of CAVs can alleviate traffic congestion significantly. When the penetration rate of CAV is low, the duration of traffic congestion is relatively long. Most vehicles on the road are HDVs, and some CAVs that follow the HDVs will degenerate from CACC to ACC driving systems. Therefore, in the case of a low penetration rate, the application of CAVs reduces the probability of congestion. However, the increase of ACC vehicles will lead to instability of traffic flow, which makes the effect of improving traffic congestion insignificant.

4.2.2. Simulation Results Based on the Car-Following Model. The micro-simulation is based on a single vehicle as to the research object, and different car-following models control the different types of vehicles. The simulation scene and simulation time are consistent with the simulation of the mixed traffic flow CTM model, which ensures the effectiveness and comparability of the model verification. The simulation results based on the car-following model are shown in Figure 8.

The speed heatmap under different CAVs penetration rates is shown in Figure 8. The bluer the color is, the slower speed and the more severe traffic congestion is. Similar to CTM simulation, the longer the traffic congestion time is, the slower the congestion dissipates under the low CAV penetration rate. With the increase of the CAV penetration rate, the duration of traffic congestion gradually decreases. This indicates that the CAVs have more advantages than the traditional HDVs in terms of traffic congestion dissipation.

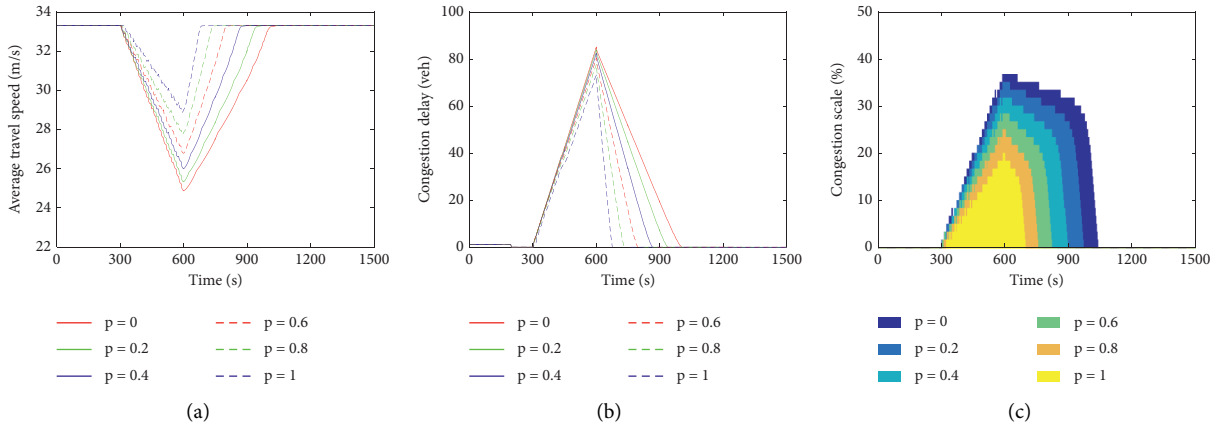

Figure 9: Traffic congestion assessment results under different CAV penetration rates: (a) average travel speed, (b) congestion delay, and (c) congestion scale.

The CTM simulation results are compared with the microscopic simulation to judge the feasibility and effectiveness of the CTM. The simulation results of the two methods are shown in Table 3. Table 3 shows that there are some differences in traffic congestion time and dissipation time under different CAV penetration rates. However, the error values of the two simulations are less than 40 s, and the maximum relative error is less than 5.89%. This means that the simulation results of the two simulations are consistent. Therefore, the simulation results show that the CTM model of mixed traffic flow is effective and feasible.

4.3. Analysis of Traffic Congestion

4.3.1. Results of Congestion Assessment. The above three congestion evaluation indexes are brought into the simulation results for the calculation. The variation law of each index under different CAV penetration rates is mined to comprehensively analyze the congestion state of mixed traffic flow. The evaluation results of congestion indexes are shown in Figure 9.

Figure 9(a) shows that due to the appearance of the bottleneck, the average travel speed under different CAV penetration rates represents a trend of first decreasing and then increasing since the simulation time of 300 s. The minimum value of average travel speed gradually decreases with the increase of CAV penetration rate. At the same time, the greater the CAV penetration rate is, the longer it takes for the average travel speed to return to the free flow speed. When the CAV penetration rate is 0, the minimum value of the average travel velocity is about 24.88 m/s, and the simulation time to recover to free flow velocity is more than 900 s. However, when the CAV penetration rate is 1, the minimum value of average travel velocity increases to 28.88 m/s, and the simulation time to recover to free flow velocity is about 700 s.

Figures 9(b) and 9(c) further report the changing trend of traffic congestion caused by mobile bottlenecks. It is demonstrated in Figures 9(b) and 9(c) that CAVs are beneficial in reducing the traffic congestion delay and congestion scale. The traffic congestion delay and congestion scale gradually decrease with the increase of the CAV penetration rate. In addition, the traffic congestion delay and congestion scale are negatively correlated with the CAV penetration rate. The higher the CAV penetration rate, the smaller the traffic congestion delay and congestion scale are. When the CAV penetration rate is 0, the roads are all HDVs, and the maximum congestion scale reaches 36.67%. On the contrary, all CACC vehicles are on the road when the penetration rate is 1, and the minimum congestion delay is reduced to 20%.

Based on the above analysis, CAVs effectively improve the traffic capacity and alleviate traffic congestion. However, different CAV penetration rates affect the index value of traffic congestion evaluation. Figure 9 shows that as the CAV penetration rate increases, the degree of traffic congestion gradually weakens, and the effect of improving traffic congestion is the best when all of them are CACC vehicles.

4.3.2. Sensitivity Analysis. In the simulation, the headway of the model parameters, traffic demand, and the duration of moving bottleneck has a certain impact on traffic congestion. Therefore, this section will conduct a sensitivity analysis of the different values of these three factors. Under the same simulation environment, three sets of simulation experiments were carried out: (1) the first group of simulation experiments is to explore the dynamic change characteristics of congestion index value with the traffic demand of 1,200 veh/h, 1,400 veh/h, and 1,600 veh/h, respectively; (2) the second group of simulation experiments is to select different headways to analyze the impact of headways of different types of vehicles on traffic congestion; and (3) the third group of simulation experiments takes into account the impact of the duration of moving bottleneck.

(1) Sensitivity Analysis of Traffic Demands. The congestion characteristics of mixed traffic flow under the traffic demand of 1,200 veh/h, 1,400 veh/h, and 1,600 veh/h are analyzed with the other experimental conditions unchanged. The congestion index values under different traffic demands are shown in Figure 10.

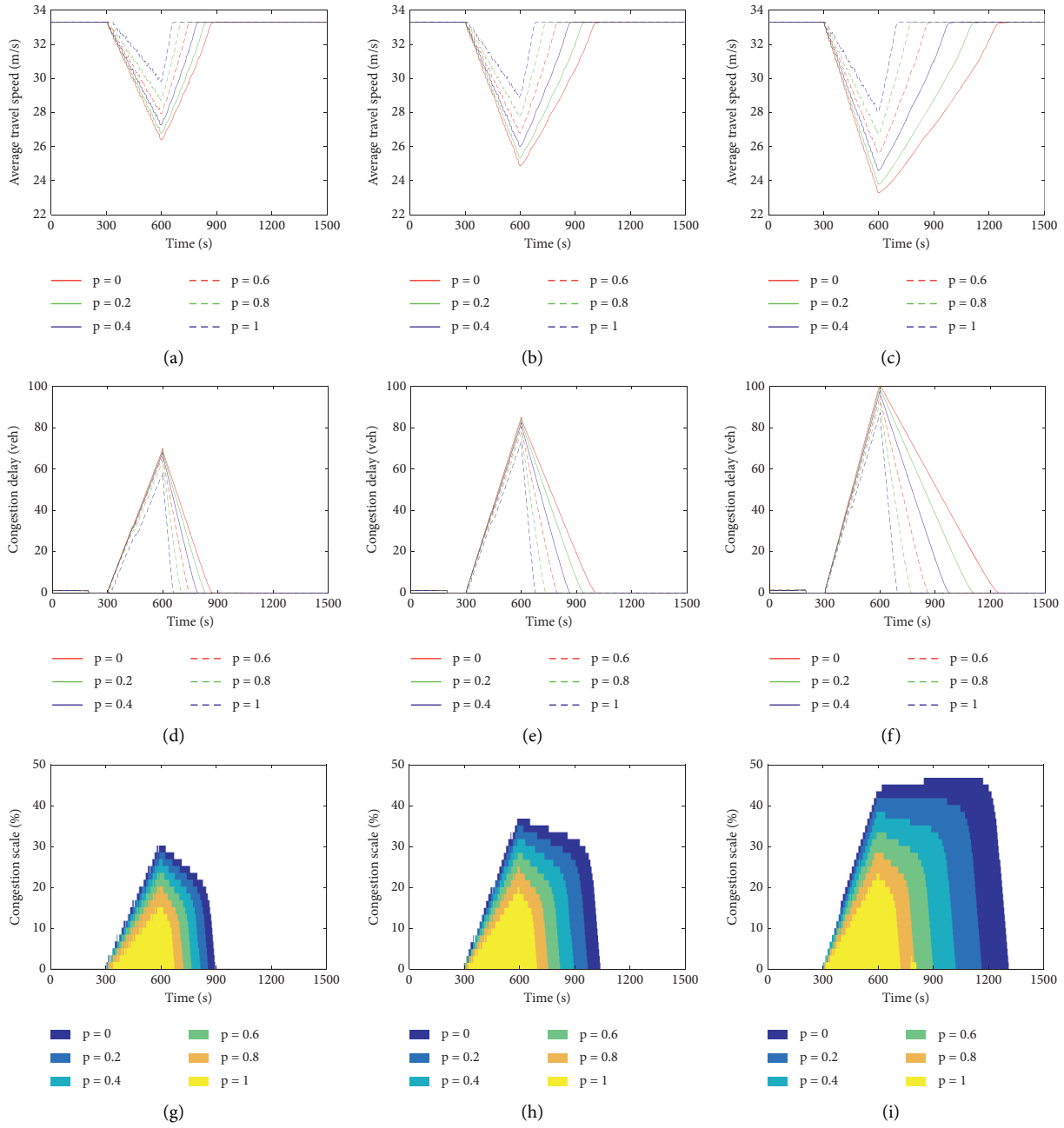

Figure 10: The results under different traffic demands: (a) average travel speed (1,200 veh/h), (b) average travel speed (1,400 veh/h), (c) average travel speed (1,600 veh/h), (d) congestion delay (1,200 veh/h), (e) congestion delay (1,400 veh/h), (f) congestion delay (1,600 veh/h), (g) congestion scale (1,200 veh/h), (h) congestion scale (1,400 veh/h), and (i) congestion scale (1,600 veh/h).

Combined with the congestion results of Section 4.2 with the traffic demand of 1,400 veh/h, the congestion index values of the three traffic demands are compared, as shown in Table 4. Under the low traffic demand of 1,200 veh/h, the congestion index value of the simulation section is small. On the one hand, when all the vehicles on the road are HDVs, the minimum average travel speed is 26.4 m/s, the maximum congestion delay is 70 veh, and the congestion scale is 30%. On the other hand, when all vehicles are CAVs, the minimum average travel speed is 29.83 m/s, the maximum congestion delay is 58 vehs, and the congestion scale is 15%. However, under the high traffic demand of 1,600 veh/h, the evaluation index of traffic congestion is more significant than that of low traffic demand. When all the vehicles on the road are HDVs, the minimum average travel speed is 23.29 m/s, the maximum congestion delay is 102 vehs, and the maximum congestion scale is 46.67%.

The comparison results show that: firstly, with the increase in traffic demand, the number of vehicles on the main highway increases gradually, and the degree of traffic congestion is more serious. Taking the CAV penetration rate $p = 0$ as an example, the congestion scale under high traffic

Table 4: Congestion indexes under different traffic demands.

Penetration rate	Traffic demand (veh/h)	Congestion indexes		
		Minimum average travel speed (m/s)	Maximum congestion delay (veh)	Maximum congestion scale (%)
0	1,200	26.4	70	30
	1,400	24.88	85	36.67
	1,600	23.29	102	46.67
0.2	1,200	26.78	69	28.33
	1,400	25.34	84	35
	1,600	23.8	100	41.67
0.4	1,200	27.27	68	26.67
	1,400	26.01	82	31.67
	1,600	24.6	98	38.33
0.6	1,200	27.94	67	23.33
	1,400	26.79	81	28.33
	1,600	25.61	95	33.33
0.8	1,200	28.73	64	20
	1,400	27.75	78	25
	1,600	26.74	92	28.33
1	1,200	29.83	58	15
	1,400	28.88	73	20
	1,600	28.04	87	23.33

demand is 16.67% higher than that under low traffic demand; the congestion delay is increased by 32 vehs; and the minimum average travel speed is increased by 3.11 m/s. Secondly, although the congestion indexes become more significant due to the increase of traffic demand when the CAV penetration rate is 1, the congestion scale under high traffic demand is only 13.33% higher than that under low traffic demand, the congestion delay is increased by 29 vehs, and the minimum average travel speed is only increased by 1.79 m/s, which indicates that CAVs slow down the growth rate of congestion caused by traffic demand.

(2) Sensitivity Analysis of Model Parameters. The expected headway of the car-following model is different, which has a certain impact on the operation of vehicles with mixed traffic flow. Therefore, the sensitivity analysis of the headway t_A and t_C will be carried out. The values of t_A is set 1.1 s, 1.6 s, and 2.2 s, respectively, and the values of t_C is set 0.6 s, 0.7 s, 0.9 s, and 1.1 s, respectively. Taking the traffic demand of 1,400 veh/h as an example, the average travel speed, traffic congestion delay, and congestion scale under different model parameters are shown in Figures 11–13, respectively.

As illustrated in Figures 11–13, the congestion index under different model parameters is slightly different in the simulation experiment, but the overall change trend is the same. The maximum value of congestion indexes under different conditions, as shown in Tables 5–7. Moreover, Figures 11(a)–11(c) show that when t_C remains unchanged, the minimum average travel speed slightly decrease as the t_A of ACC vehicles increases. From Figures 11(a), 11(d), 11(g), and 11(j), it can be seen that when t_A is unchanged, the minimum average travel speed decreases as the t_C of CACC vehicle increases.

Similarly, as seen in Figures 12(a)–12(c) and Figures 13(a)–13(c), when t_C does not change, taking $t_c = 0.6s$ as an example, the difference between the maximum congestion delay under different t_A is no more than 2 vehs. And the difference between the maximum congestion scale is no more than 5%. Moreover, Figures 12(a), 12(d), 12(g), 12(j), 13(a), 13(d), 13(g), and 13(j) indicate that when t_C remains unchanged, taking $t_A = 1.1s$ as an example, the congestion delay does not exceed 8 vehs with the increase in t_C. And the congestion scale does not exceed 8.33%. However, all indexes decrease with the increase in CAVs penetration rate. This means that the difference in traffic congestion evaluation index caused by different model parameters accounts for a low proportion of itself. Therefore, the difference in model parameters has little effect on the overall evaluation results of traffic congestion.

The comparison of the results of different model parameters shows that the headway of CAVs has a slight impact on the average travel speed, congestion delay, and congestion delay of mixed traffic flow under different model parameters. This indicates that the shorter the headway of CAVs, the more sensitive to the dissipation of traffic congestion. However, the trend of congestion index change is the same as the overall level. With the increase in the penetration rate, traffic congestion is significantly reduced. The result suggests that CAVs are conducive to improving traffic congestion.

(3) Sensitivity Analysis of Bottleneck Duration. The characteristics of traffic flow on expressways under the duration of 100 s, 200 s, and 300 s are studied, respectively. The traffic demand is set as 1,400 veh/h, and the model parameters are set as $t_A = 1.1s$ and $t_C = 0.6s$. The duration of the moving bottleneck starting from the simulation time 300 s is adjusted to be 100 s, 200 s, and 300 s, respectively. The congestion indexes of the simulation experiment are shown in Figure 14.

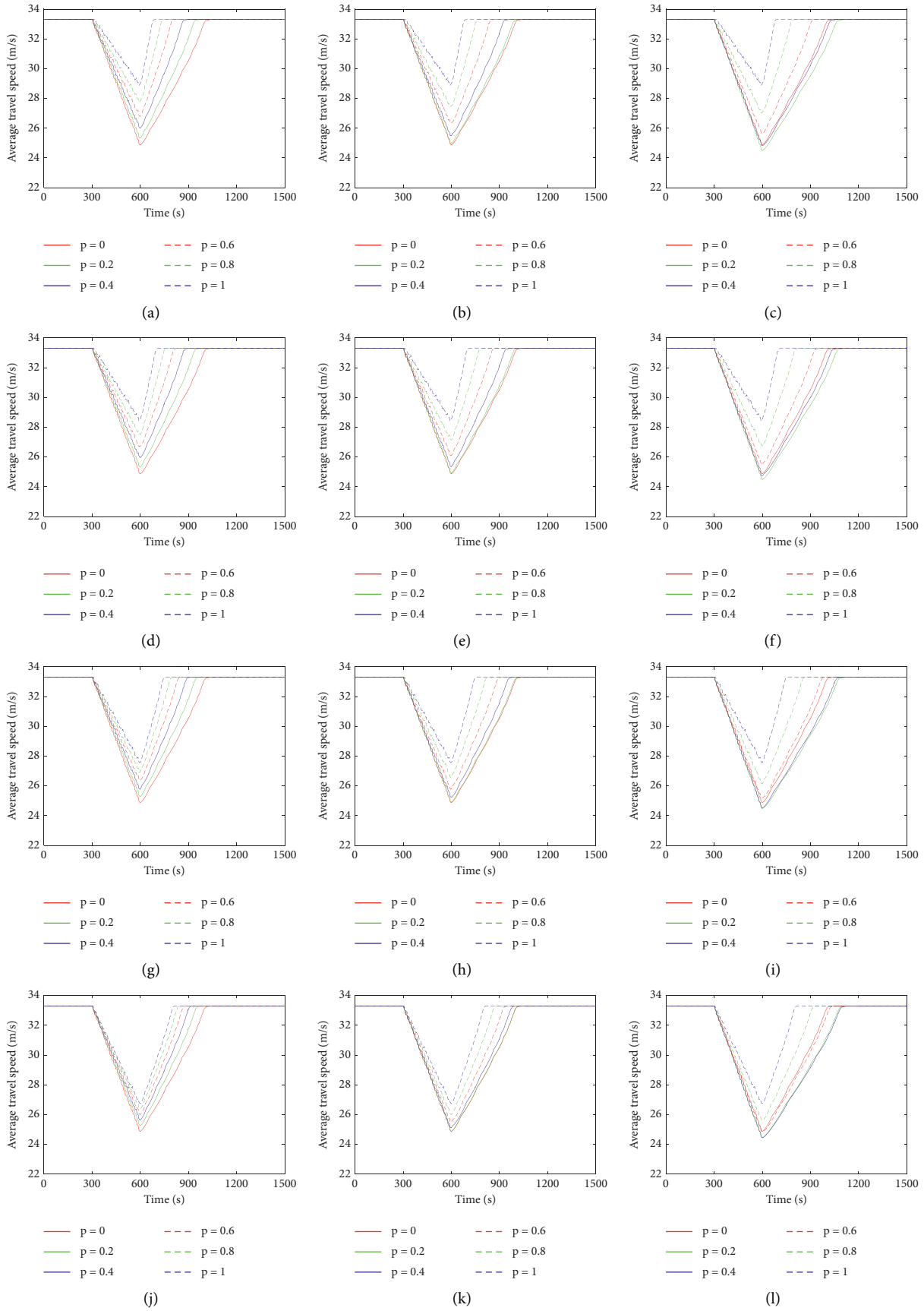

FIGURE 11: Average travel speed under different model parameters: (a) $t_A = 1.1, t_C = 0.6$, (b) $t_A = 1.6, t_C = 0.6$, (c) $t_A = 2.2, t_C = 0.6$, (d) $t_A = 1.1, t_C = 0.7$, (e) $t_A = 1.6, t_C = 0.7$, (f) $t_A = 2.2, t_C = 0.7$, (g) $t_A = 1.1, t_C = 0.9$, (h) $t_A = 1.6, t_C = 0.9$, (i) $t_A = 2.2, t_C = 0.9$, (j) $t_A = 1.1, t_C = 1.1$, (k) $t_A = 1.6, t_C = 1.1$, and (l) $t_A = 2.2, t_C = 1.1$.

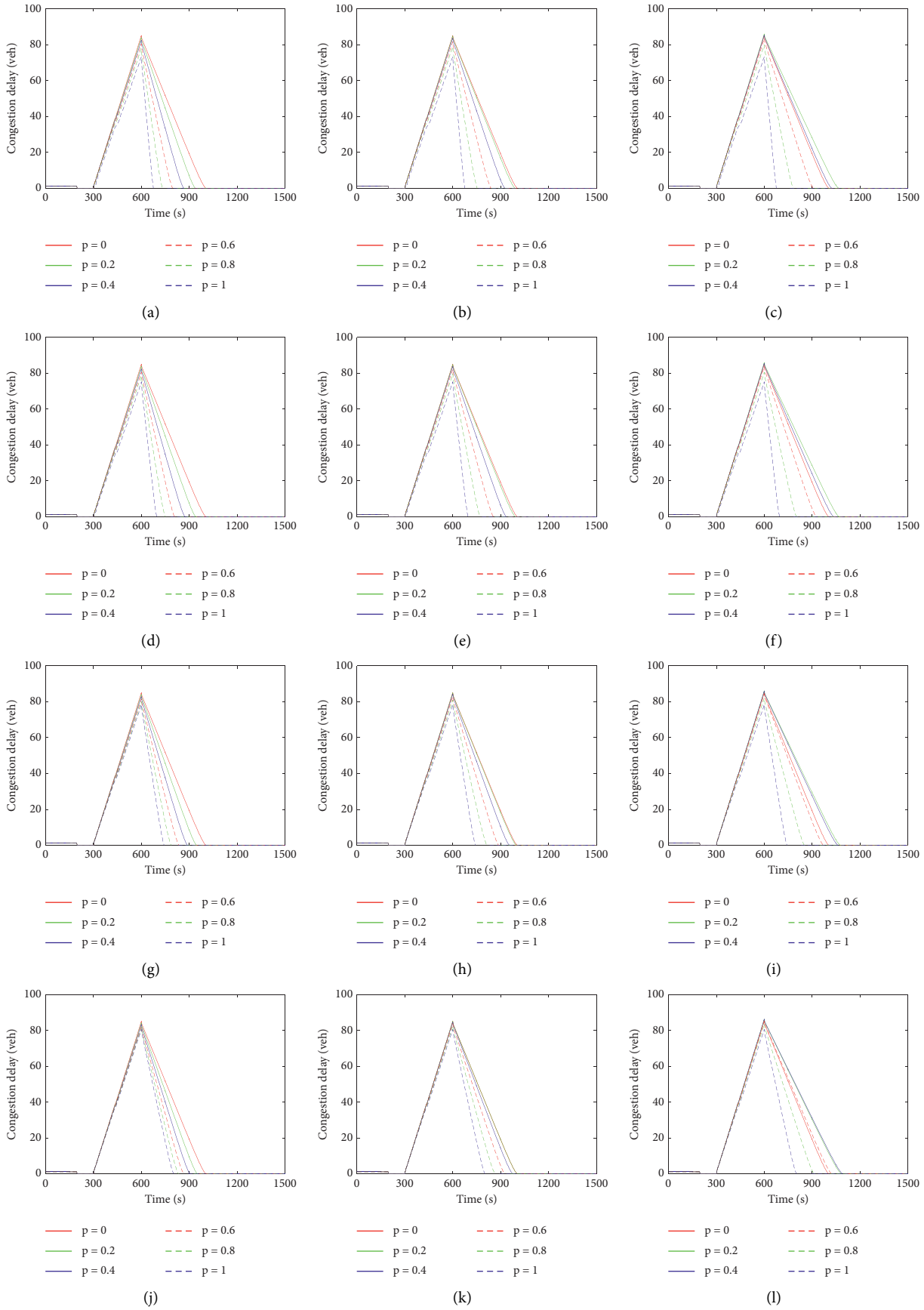

FIGURE 12: Traffic congestion delay under different model parameters: (a) $t_A = 1.1, t_C = 0.6$, (b) $t_A = 1.6, t_C = 0.6$, (c) $t_A = 2.2, t_C = 0.6$, (d) $t_A = 1.1, t_C = 0.7$, (e) $t_A = 1.6, t_C = 0.7$, (f) $t_A = 2.2, t_C = 0.7$, (g) $t_A = 1.1, t_C = 0.9$, (h) $t_A = 1.6, t_C = 0.9$, (i) $t_A = 2.2, t_C = 0.9$, (j) $t_A = 1.1, t_C = 1.1$, (k) $t_A = 1.6, t_C = 1.1$, and (l) $t_A = 2.2, t_C = 1.1$.

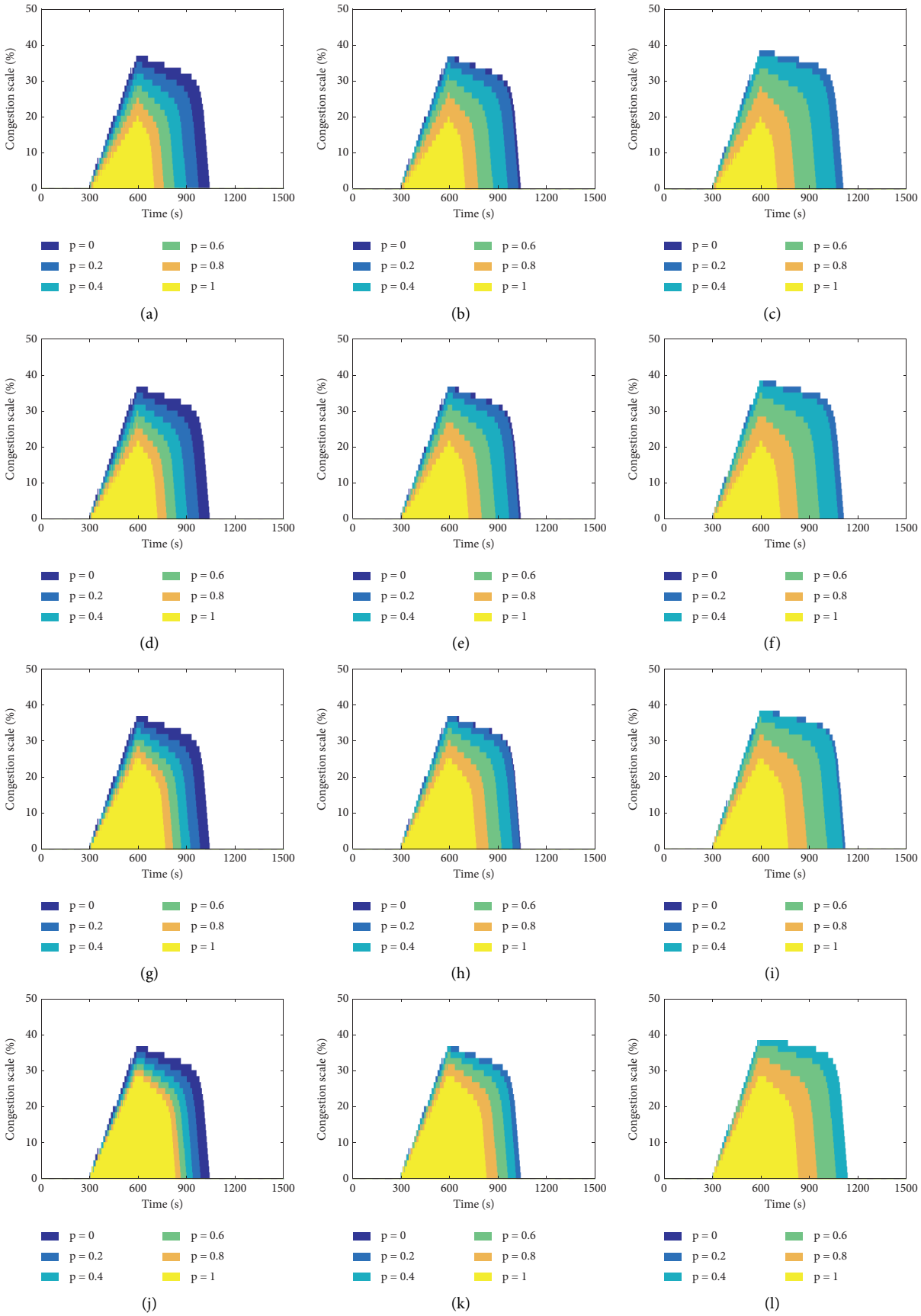

Figure 13: Congestion scale under different model parameters: (a) $t_A = 1.1, t_C = 0.6$, (b) $t_A = 1.6, t_C = 0.6$, (c) $t_A = 2.2, t_C = 0.6$, (d) $t_A = 1.1, t_C = 0.7$, (e) $t_A = 1.6, t_C = 0.7$, (f) $t_A = 2.2, t_C = 0.7$, (g) $t_A = 1.1, t_C = 0.9$, (h) $t_A = 1.6, t_C = 0.9$, (i) $t_A = 2.2, t_C = 0.9$, (j) $t_A = 1.1, t_C = 1.1$, (k) $t_A = 1.6, t_C = 1.1$, and (l) $t_A = 2.2, t_C = 1.1$.

Table 5: Maximum value of $\overline{v}$ under different model parameters (unit: m/s).

Model parameters	0	0.2	0.4	0.6	0.8	1
$t_A = 1.1s, t_C = 0.6s$	24.88	25.34	26.01	26.79	27.75	28.88
$t_A = 1.1s, t_C = 0.7s$	24.88	25.32	25.97	26.71	27.50	28.43
$t_A = 1.1s, t_C = 0.9s$	24.88	25.29	25.78	26.36	26.91	27.57
$t_A = 1.1s, t_C = 1.1s$	24.88	25.26	25.63	26.01	26.38	26.74
$t_A = 1.6s, t_C = 0.6s$	24.88	24.96	25.49	26.36	27.44	28.88
$t_A = 1.6s, t_C = 0.7s$	24.88	24.94	25.36	26.10	27.14	28.43
$t_A = 1.6s, t_C = 0.9s$	24.88	24.91	25.24	25.78	26.58	27.57
$t_A = 1.6s, t_C = 1.1s$	24.88	24.88	25.12	25.49	26.01	26.74
$t_A = 2.2s, t_C = 0.6s$	24.88	24.50	24.82	25.62	27.01	28.88
$t_A = 2.2s, t_C = 0.7s$	24.88	24.49	24.73	25.49	26.74	28.43
$t_A = 2.2s, t_C = 0.9s$	24.88	24.47	24.52	25.21	26.14	27.57
$t_A = 2.2s, t_C = 1.1s$	24.88	24.45	24.44	24.82	25.60	26.74

Table 6: Maximum congestion delay under different model parameters (unit: vehs).

Model parameters	0	0.2	0.4	0.6	0.8	1
$t_A = 1.1s, t_C = 0.6s$	85	84	82	81	78	73
$t_A = 1.1s, t_C = 0.7s$	85	84	82	81	78	75
$t_A = 1.1s, t_C = 0.9s$	85	84	83	82	80	79
$t_A = 1.1s, t_C = 1.1s$	85	84	83	82	82	81
$t_A = 1.6s, t_C = 0.6s$	85	85	84	82	79	73
$t_A = 1.6s, t_C = 0.7s$	85	85	84	82	80	75
$t_A = 1.6s, t_C = 0.9s$	85	85	84	83	81	79
$t_A = 1.6s, t_C = 1.1s$	85	85	85	84	82	81
$t_A = 2.2s, t_C = 0.6s$	85	86	85	83	80	73
$t_A = 2.2s, t_C = 0.7s$	85	86	86	84	81	75
$t_A = 2.2s, t_C = 0.9s$	85	86	86	85	82	79
$t_A = 2.2s, t_C = 1.1s$	85	86	86	85	84	81

Table 7: Maximum congestion scale under different model parameters (unit: %).

Model parameters	0	0.2	0.4	0.6	0.8	1
$t_A = 1.1s, t_C = 0.6s$	36.67	35.00	31.67	28.33	25.00	20.00
$t_A = 1.1s, t_C = 0.7s$	36.67	35.00	31.67	30.00	26.67	21.67
$t_A = 1.1s, t_C = 0.9s$	36.67	35.00	33.33	30.00	28.33	25.00
$t_A = 1.1s, t_C = 1.1s$	36.67	35.00	33.33	31.67	30.00	28.33
$t_A = 1.6s, t_C = 0.6s$	36.67	36.67	35.00	31.67	26.67	20.00
$t_A = 1.6s, t_C = 0.7s$	36.67	36.67	35.00	31.67	26.67	21.67
$t_A = 1.6s, t_C = 0.9s$	36.67	36.67	35.00	33.33	30.00	25.00
$t_A = 1.6s, t_C = 1.1s$	36.67	36.67	36.67	35.00	31.67	28.33
$t_A = 2.2s, t_C = 0.6s$	36.67	38.33	36.67	33.33	28.33	20.00
$t_A = 2.2s, t_C = 0.7s$	36.67	38.33	38.33	35.00	28.33	21.67
$t_A = 2.2s, t_C = 0.9s$	36.67	38.33	38.33	36.67	31.67	25.00
$t_A = 2.2s, t_C = 1.1s$	36.67	38.33	38.33	36.67	33.33	28.33

Figure 14 reports that the average travel speed, congestion delay, and congestion scale are changed under the different duration of moving bottlenecks. When the moving bottleneck occurs, the average travel speed is negatively correlated with the degree of duration, while the congestion delay, the scale of congestion, and the degree of duration show a positive correlation growth trend. When the duration is 100s, the impact of moving bottleneck on traffic is significantly reduced. The average travel speed under different CAV penetration rates is within 30 m/s, while the maximum congestion delay is 29 vehs and the maximum congestion scale is 13.3%. When the duration is 200 s, the minimum average travel speed of the overall traffic flow increases to 27.64 m/s, the maximum congestion delay is 56 vehs, and the maximum congestion scale is 25%. When the duration is 300 s, the moving bottleneck has the most significant impact on traffic. The minimum average travel speed is 24.88 m/s, while the maximum congestion delay reaches 85 vehs and the maximum congestion scale increases to 36.67%.

The above analysis shows that the duration of the moving bottleneck is closely related to traffic congestion. The longer the duration is, the more serious the traffic congestion caused. When the duration is 300 s, and the CAVs penetration rate is 0, the minimum average travel speed is 5.54 m/s greater than that of the duration of 100 s, while the maximum congestion delay increases by about 1.93 than that

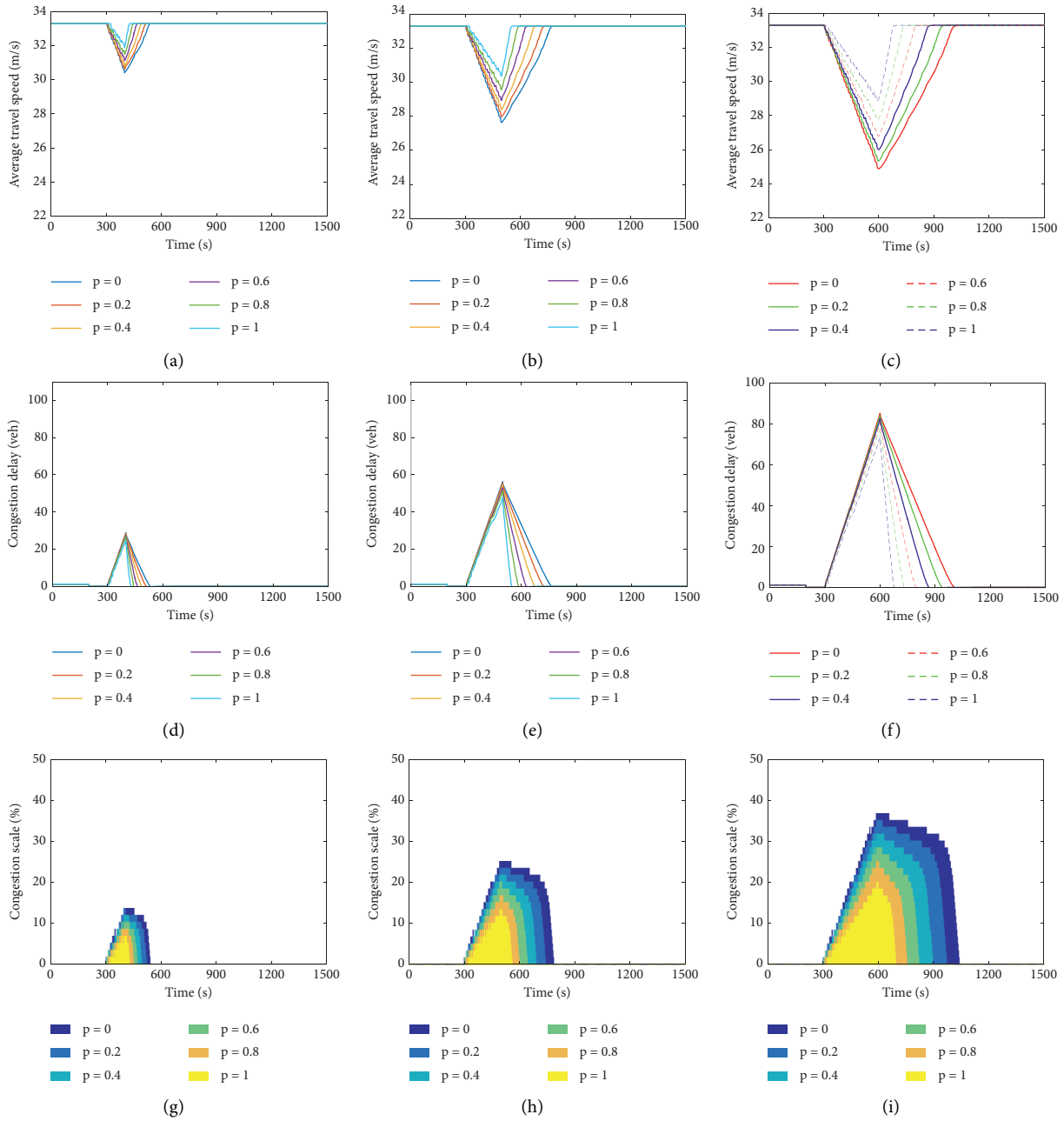

Figure 14: Traffic congestion indexes under different bottleneck duration: (a) average travel speed (100 s), (b) average travel speed (200 s), (c) average travel speed (300 s), (d) congestion delay (100 s), (e) congestion delay (200 s), (f) congestion delay (300 s), (g) congestion scale (100 s), (h) congestion scale (200 s), and (i) congestion scale (300 s).

of the duration of 100 s, and the maximum congestion scale is approximately 1.75 times higher than that in the case of a duration of 100 s. However, with the increase in CAV penetration rate, the growth rate of congestion indexes has gradually slowed down.

5. Conclusions and Future Work

5.1. Conclusions. This study proposed a cell transmission model to simulate traffic congestion for mixed flow with connected automated vehicles and human-driven vehicles. Based on the simulation, some conclusions are drawn as follows:

(1) The maximum capacity achieved in the full CACCs environment is greater than the maximum capacity in the full ACCs and full HDVs environment. When the CAVs penetration rate is 0, 0.2, 0.4, 0.6, 0.8, and 1, the maximum capacity of mixed traffic flow under high CAV penetration rates is higher, which indicates that the CAVs effectively improve the road traffic efficiency.

(2) By the comparison between meso- and micro-simulation methods, it is found that the simulation results of the two methods are consistent. The error of both methods is less than 40 s, and the maximum relative error of both methods is less than 5.89%, which indicates that the CTM model of mixed traffic flow is effective and feasible.

(3) The average travel speed, congestion delay, and congestion scale decrease with the increase in CAV penetration rate.

(4) The traffic congestion caused by high traffic demand and the long duration of mobile bottleneck is more and more serious.

(5) The congestion index is slightly different under different model parameters, but the degree of congestion is still significantly reduced when the CAVs penetration rate exceeds 0.8.

(6) The traffic demand and the duration of the moving bottleneck are closely related to the congestion assessment, while the model parameters have little effect on the traffic congestion.

5.2. Future Work. To model and simulate the mixed traffic flow with HDVs and CAVs, this paper proposed a CTM model based on the fundamental diagram of mixed traffic flow under different CAV penetration rates. There are still some problems that need further study. First of all, we only consider the car following behavior. In the future, we will introduce lane-changing behavior to make it closer to the actual traffic flow. Moreover, CAVs can realize platoon driving by lane-changing to further improve traffic capacity and traffic congestion. Therefore, the influence of the behavior of the CAVs platoon will be further studied in the future.

Data Availability

The simulation data used to support the findings of this study are included within the article.

Conflicts of Interest

The authors declare conflicts of interest.

Acknowledgments

The paper received research funding support from the National Natural Science Foundation of China (52002339), the Sichuan Science and Technology Program (2021YJ0535 and 2022YFG0152), the Fundamental Research Funds for the Central Universities (2682021CX058), and the Guangxi Science and Technology Program (2021AA01007AA).

References

[1] M. Pourmehrab, L. Elefteriadou, S. Ranka, and M. Martin-Gasulla, "Optimizing signalized intersections performance under conventional and automated vehicles traffic," *IEEE Transactions on Intelligent Transportation Systems*, vol. 21, no. 7, pp. 2864–2873, 2020.

[2] Y. Yang, K. He, Y.-P. Wang, Z.-Z. Yuan, Y.-h. Yin, and M.-z. Guo, "Identification of dynamic traffic crash risk for cross-area freeways based on statistical and machine learning methods," *Physica A: Statistical Mechanics and Its Applications*, vol. 595, Article ID 127083, 2022.

[3] Z. Yao, Y. Jiang, B. Zhao, X. Luo, and B. Peng, "A dynamic optimization method for adaptive signal control in a connected vehicle environment," *Journal of Intelligent Transportation Systems*, vol. 24, no. 2, pp. 184–200, 2020.

[4] Z. Yao, L. Shen, R. Liu, Y. Jiang, and X. Yang, "A dynamic predictive traffic signal control framework in a cross-sectional vehicle infrastructure integration environment," *IEEE Transactions on Intelligent Transportation Systems*, vol. 21, no. 4, p. 12, 2020.

[5] C. Yu, Y. Feng, H. X. Liu, W. Ma, and X. Yang, "Integrated optimization of traffic signals and vehicle trajectories at isolated urban intersections," *Transportation Research Part B: Methodological*, vol. 112, pp. 89–112, 2018.

[6] C. Chen, J. Wang, Q. Xu, J. Wang, and K. Li, "Mixed platoon control of automated and human-driven vehicles at a signalized intersection: dynamical analysis and optimal control," *Transportation Research Part C: Emerging Technologies*, vol. 127, Article ID 103138, 2021.

[7] Y. Jiang, S. Wang, Z. Yao, B. Zhao, and Y. Wang, "A cellular automata model for mixed traffic flow considering the driving behavior of connected automated vehicle platoons," *Physica A: Statistical Mechanics and Its Applications*, vol. 582, Article ID 126262, 2021a.

[8] Y. Jiang, B. Zhao, M. Liu, and Z. Yao, "A two-level model for traffic signal timing and trajectories planning of multiple CAVs in a random environment," *Journal of Advanced Transportation*, vol. 2021, Article ID 9945398, 13 pages, 2021.

[9] X. T. Yang, K. Huang, Z. Zhang, Z. A. Zhang, and F. Lin, "Eco-driving system for connected automated vehicles: multi-objective trajectory optimization," *IEEE Transactions on Intelligent Transportation Systems*, vol. 22, no. 99, pp. 1–13, 2020.

[10] Z. Yao, H. Jiang, Y. Cheng, Y. Jiang, and B. Ran, "Integrated schedule and trajectory optimization for connected automated vehicles in a conflict zone," *IEEE Transactions on Intelligent Transportation Systems*, vol. 23, no. 3, pp. 1841–1851, 2022.

[11] V.-T. Ta and A. Dvir, "A secure road traffic congestion detection and notification concept based on V2I communications," *Vehicular Communications*, vol. 25, Article ID 100283, 2020.

[12] M. A. Raposo, M. Grosso, A. Mourtzouchou, J. Krause, A. Duboz, and B. Ciuffo, "Research in transportation economics economic implications of a connected and automated mobility in Europe," *Research in Transportation Economics*, vol. 92, Article ID 101072, 2021.

[13] L. Ye and T. Yamamoto, "Evaluating the impact of connected and autonomous vehicles on traffic safety," *Physica A: Statistical Mechanics and Its Applications*, vol. 526, Article ID 121009, 2019.

[14] Y.-M. Yuan, R. Jiang, M.-B. Hu, Q.-S. Wu, and R. Wang, "Traffic flow characteristics in a mixed traffic system consisting of ACC vehicles and manual vehicles: a hybrid modelling approach," *Physica A: Statistical Mechanics and Its Applications*, vol. 388, no. 12, pp. 2483–2491, 2009.

[15] H. B. Zhu, Y. J. Zhou, and W. J. Wu, "Modeling traffic flow mixed with automated vehicles considering drivers ' character

difference," *Physica A: Statistical Mechanics and Its Applications*, vol. 549, 2020.

[16] M. Bando, K. Hasebe, A. Nakayama, A. Shibata, and Y. Sugiyama, "Dynamical model of traffic congestion and numerical simulation," *Physical Review A*, vol. 51, no. 2, pp. 1035–1042, 1995.

[17] D. C. Gazis, R. Herman, and R. W. Rothery, "Nonlinear follow-the-leader models of traffic flow," *Operations Research*, vol. 9, no. 4, pp. 545–567, 1961.

[18] G. F. Newell, "A simplified car-following theory: a lower order model," *Transportation Research Part B: Methodological*, vol. 36, no. 3, pp. 195–205, 2002a.

[19] P. I. Richards, "Shock waves on the highway," *Operations Research*, vol. 4, no. 1, pp. 42–51, 1956.

[20] C. F. Daganzo, "The cell transmission model: a dynamic representation of highway traffic consistent with the hydrodynamic theory," *Transportation Research Part B: Methodological*, vol. 28, no. 4, pp. 269–287, 1994.

[21] C. F. Daganzo, "The cell transmission model, part II: network traffic," *Transportation Research Part B: Methodological*, vol. 29, no. 2, pp. 79–93, 1995.

[22] H. Dong, S. Ma, M. Guo, and D. Liu, "Research on analysis method of traffic congestion mechanism based on improved cell transmission model," *Discrete Dynamics in Nature and Society*, vol. 2012, Article ID 854654, 11 pages, 2012.

[23] M. Carey, C. Balijepalli, and D. Watling, "Extending the cell transmission model to multiple lanes and lane-changing," *Networks and Spatial Economics*, vol. 15, no. 3, pp. 507–535, 2015.

[24] C. Canudas-de-Wit and A. Ferrara, "A variable-length Cell Transmission Model for road traffic systems," *Transportation Research Part C: Emerging Technologies*, vol. 97, pp. 428–455, 2018.

[25] Z. Qian, J. Li, X. Li, M. Zhang, and H. Wang, "Modeling heterogeneous traffic flow: a pragmatic approach," *Transportation Research Part B: Methodological*, vol. 99, pp. 183–204, 2017.

[26] G. Qian, M. Guo, L. Zhang, Y. Wang, S. Hu, and D. Wang, "Traffic scheduling and control in fully connected and automated networks," *Transportation Research Part C: Emerging Technologies*, vol. 126, Article ID 103011, 2021.

[27] Y. Qin, H. Wang, and D. Ni, "LWR model for traffic flow mixed with CACC vehicles," *Transportation Science:trsc*, vol. 55, p. 1057, 2021.

[28] H. Yao and X. Li, "Decentralized control of connected automated vehicle trajectories in mixed traffic at an isolated signalized intersection," *Transportation Research Part C: Emerging Technologies*, vol. 121, Article ID 102846, 2020.

[29] Z. Yao, T. Xu, Y. Jiang, and R. Hu, "Linear stability analysis of heterogeneous traffic flow considering degradations of connected automated vehicles and reaction time," *Physica A: Statistical Mechanics and Its Applications*, vol. 561, Article ID 125218, 2021.

[30] J. Zhou and F. Zhu, "Modeling the fundamental diagram of mixed human-driven and connected automated vehicles," *Transportation Research Part C: Emerging Technologies*, vol. 115, Article ID 102614, 2020.

[31] F. Zheng, C. Liu, X. Liu, S. E. Jabari, and L. Lu, "Analyzing the impact of automated vehicles on uncertainty and stability of the mixed traffic flow," *Transportation Research Part C: Emerging Technologies*, vol. 112, pp. 203–219, 2020.

[32] Y. Qin, H. Wang, and W. Wang, "Analysis on stability and safety for mixed traffic flow with connected auxiliary driving," *Dongnan Daxue Xuebao (Ziran Kexue Ban)/Journal of Southeast University (Natural Science Edition)*, vol. 48, no. 1, pp. 188–194, 2018.

[33] Y. Y. Qin, H. Wang, and B. Ran, "Car-following model of connected and autonomous vehicles considering multiple feedbacks," *Jiaotong Yunshu Xitong Gongcheng Yu Xinxi/Journal of Transportation Systems Engineering and Information Technology*, vol. 18, no. 3, pp. 48–54, 2018.

[34] Y. Y. Qin, H. Wang, W. Wang, and Q. Wan, "Mixed traffic flow string stability analysis for different CACC penetration ranges," *Jiaotong Yunshu Xitong Gongcheng Yu Xinxi/Journal of Transportation Systems Engineering and Information Technology*, vol. 17, no. 4, 2017.

[35] Y. Jiang, R. Hu, Z. Yao, P. Wu, and X. Luo, "Stability and safety for heterogeneous traffic flow composed of intelligent and connected vehicles," *Journal of Beijing Jiaotong University*, vol. 44, no. 1, pp. 27–33, 2020.

[36] M. Ramezani and E. Ye, "Lane density optimisation of automated vehicles for highway congestion control," *Transportation Business: Transport Dynamics*, vol. 7, no. 1, pp. 1096–1116, 2019.

[37] T. Xu, Z. Yao, Y. Jiang, and T. Yang, "Fundamental Diagram Model of Considering Reaction Time in Environment of Intelligent Connected Vehicles," *Gonglu Jiaotong Keji/Journal of Highway and Transportation Research and Development*, vol. 37, 2020.

[38] R. Jiang, Q. Wu, and Z. Zhu, "Full velocity difference model for a car-following theory," *Physical Review E: Statistical, Nonlinear, and Soft Matter Physics*, vol. 64, no. 1, Article ID 017101, 2001.

[39] M. Treiber, A. Hennecke, and D. Helbing, "Congested traffic states in empirical observations and microscopic simulations," *Physical Review A*, vol. 62, no. 2, pp. 1805–1824, 2000.

[40] C. Shirke, A. Bhaskar, and E. Chung, "Macroscopic modelling of arterial traffic: an extension to the cell transmission model," *Transportation Research Part C: Emerging Technologies*, vol. 105, pp. 54–80, 2019.

[41] V. Milanés and S. E. Shladover, "Modeling cooperative and autonomous adaptive cruise control dynamic responses using experimental data," *Transportation Research Part C: Emerging Technologies*, vol. 48, pp. 285–300, 2014.

[42] S. E. Shladover, D. Su, and X.-Y. Lu, "Impacts of cooperative adaptive cruise control on freeway traffic flow," *Transportation Research Record: Journal of the Transportation Research Board*, vol. 2324, no. 1, pp. 63–70, 2012.

[43] Z. Yao, R. Hu, Y. Jiang, and T. Xu, "Stability and safety evaluation of mixed traffic flow with connected automated vehicles on expressways," *Journal of Safety Research*, vol. 75, pp. 262–274, 2020.

[44] Z. Yao, R. Hu, Y. Wang, Y. Jiang, B. Ran, and Y. Chen, "Stability analysis and the fundamental diagram for mixed connected automated and human-driven vehicles," *Physica A: Statistical Mechanics and Its Applications*, vol. 533, Article ID 121931, 2019.

[45] A. Mohan Rao and K. Ramachandra Rao, "Measuring urban traffic congestion - a review," *International Journal of Traffic and Transportation Engineering*, vol. 2, no. 4, pp. 286–305, 2012.